参赛队员姓名：<u>Grace Qiao</u>

中学：<u>北京师范大学附属实验中学</u>

省份：<u>北京</u>

国家/地区：<u>中国</u>

指导教师姓名：<u>和亚宁、孔婀静</u>

指导教师单位：<u>清华大学、北京师范大学附属实验中学国际部</u>

论文题目：**Hyaluronic Acid-Based Azo Polymer: Synthesis, Characterization and Potential Application in Biomedical Field**

Hyaluronic Acid-Based Azo Polymer: Synthesis, Characterization and Potential Application in Biomedical Field

Grace Qiao

Abstract

This study aimed to synthesize a hyaluronic acid-based azobenzene polymer with a high grafting ratio and redox-responsiveness. Hyaluronic acid was successfully grafted with azobenzene by reacting with a diazonium salt derived from aminobenzoic acid through azo-coupling. By using the ^{1}H NMR spectroscopy, we showed that the final product achieved a grafting ratio of approximately 75%. The azobenzene-modified hyaluronic acid was allowed to self-assemble in a selected solvent (DMSO/H_2O) to produce uniform colloidal spheres, which were subsequently characterized by dynamic light scattering instrument and transmission electron microscopy. UV-Vis spectrum demonstrated that the azobenzene groups could be efficiently reduced by sodium dithionite, confirming the polymer's redox-responsiveness. Amine-functionalized tetraphenylethene and fluorescence spectroscopy were employed to simulate a successful payload release from the polymer. The azobenzene-modified hyaluronic acid synthesized in this study enhanced the value of hyaluronic acid and suggested the potential applications for tumor cell-targeted drug carriers.

**Keywords**: azobenzene, hyaluronic acid, azo-coupling, redox-responsiveness, tumor cell targeting.

Table of Contents

1. Introduction

Natural polysaccharide-based polymers, such as chitosan, cellulose, and hyaluronic acid, are abundant in nature. They offer benefits such as biodegradability, biocompatibility, reactivity, affordability, and high annual production, making them suitable alternatives to some petroleum-based polymers. While the annual production of these polysaccharide polymers is substantial—cellulose production, for instance, can reach 10^{12} tons—only 0.2% is effectively utilized. [1] Therefore, functionalizing polysaccharide polymers and enhancing the value of their products are effective means to promote the development of this industry.

Hyaluronic acid (see Figure 1.1) is a linear polysaccharide composed of repeating disaccharide units, *N*-acetyl-D-glucosamine and D-glucuronide, linked together by alternating β-1,3 and β-1,4 glycosidic bonds. [2] Among various polysaccharide materials, hyaluronic acid is known for its superior degradability, biocompatibility, tumor cell targeting ability, and reactivity. Thus, it is a highly promising polysaccharide polymer and the central focus of this study. [3]
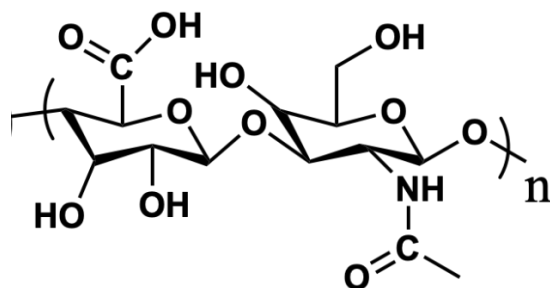
[1] Klemm, D., Heublein, B., Fink, H. P., & Bohn, A. (2005, May 30). Cellulose: Fascinating Biopolymer and Sustainable Raw Material. Angewandte Chemie International Edition, 44(22), 3358–3393.

[2] Bicudo, R. C. S., & Santana, M. H. A. (2012, March 1). Effects of Organic Solvents on Hyaluronic Acid Nanoparticles Obtained by Precipitation and Chemical Crosslinking. Journal of Nanoscience and Nanotechnology, 12(3), 2849–2857.

[3] Luo, Z., Dai, Y., & Gao, H. (2019, November). Development and application of hyaluronic acid in tumor targeting drug delivery. Acta Pharmaceutica Sinica B, 9(6), 1099–1112.

Figure 1.1: Structure of Hyaluronic Acid

Enhancing the value of a material often involves modifying it to be stimuli-responsive. Stimuli-responsive polymers possess the capacity to alter their physical or chemical characteristics in response to their surrounding environment, facilitating various essential functionalities. These responses can be triggered by various factors, including changes in pH, temperature, and electrolyte concentration. Non-invasive and easily controllable triggers, such as light, electricity, magnetism, and acoustic fields, are also highly promising. Additionally, there are stimuli that are specific to biological systems, like the oxygen-depleted (hypoxic) microenvironments of tumor cells, specific antigen-antibody interactions, reductases, and glucose levels. Materials that are capable of responding to the triggers mentioned can have broad potential applications in the biomedical fields.[4,5,6] Currently, areas of intense research focus for stimuli-responsive materials encompass drug delivery systems, bioimaging, tissue repair, biosensing, and optical information storage.[7] The aim of this study lies on exploring the potential application of stimuli-responsive polymers in tumor cell-targeted drug delivery systems.

Cancer treatment remains a significant challenge in biomedicine, encompassing chemotherapy, radiotherapy, and surgery. Among these, chemotherapy can exert severe side effects on patients as

---

[4] Roy, D., Cambre, J. N., & Sumerlin, B. S. (2010, January). Future perspectives and recent advances in stimuli-responsive materials. Progress in Polymer Science, 35(1–2), 278–301.

[5] Wei, M., Gao, Y., Li, X., & Serpe, M. J. (2017). Stimuli-responsive polymers and their applications. Polymer Chemistry, 8(1), 127–143.

[6] Bawa, P., Pillay, V., Choonara, Y. E., & du Toit, L. C. (2009, March 5). Stimuli-responsive polymers and their applications in drug delivery. Biomedical Materials, 4(2), 022001.

[7] Stuart, M. A. C., Huck, W. T. S., Genzer, J., Müller, M., Ober, C., Stamm, M., Sukhorukov, G. B., Szleifer, I., Tsukruk, V. V., Urban, M., Winnik, F., Zauscher, S., Luzinov, I., & Minko, S. (2010, January 22). Emerging applications of stimuli-responsive polymer materials. Nature Materials, 9(2), 101–113.

it indiscriminately attacks cells throughout the body. One of the main tools to mitigate this issue is the development of targeted cancer drugs. The mechanism behind targeted cancer drugs involves encapsulating the drugs in stimuli-responsive carriers, and these carriers are designed to be activated by specific triggers present at tumor sites, prompting them to release a drug selectively. This strategy holds promise for directing precise attacks on tumor cells. By employing effective targeted drug carriers, it is possible to both diminish the side effects of chemotherapeutic agents and enhance their efficacy.

Tumor cells proliferate rapidly, leading to an oxygen-depleted cellular microenvironment with an overexpression of various reductase enzymes. Research have shown that hypoxia can induce drug resistance, thereby undermining therapeutic efficacy.[8] Nano drug carriers that respond to hypoxia or redox changes can leverage this characteristic that is unique to tumor cells, enabling controlled drug release precisely at tumor sites. Thus, developing hypoxia or redox-responsive polymers holds great importance in the field of cancer therapy.

Azobenzene is among the most well-known substances used to endow polymers with redox-responsiveness. Its synthesis is straightforward, and its structural diversity offers unique advantages. In a reducing environment, the nitrogen-nitrogen double bond in azobenzene is cleaved, forming two amino groups. This cleavage disrupts the material's overall structure, facilitating functions such as drug delivery (see Figure 1.2). Therefore, azobenzene holds unique

---

[8] Wilson, W. R., & Hay, M. P. (2011, May 24). Targeting hypoxia in cancer therapy. Nature Reviews Cancer, 11(6), 393–410.

potential in the development of targeted cancer drug carriers. Merging the targeting ability of hyaluronic acid with the redox-responsiveness of azobenzene not only enhances the value and functionality of hyaluronic acid products but also provides insights in the research of targeted cancer drug delivery systems.
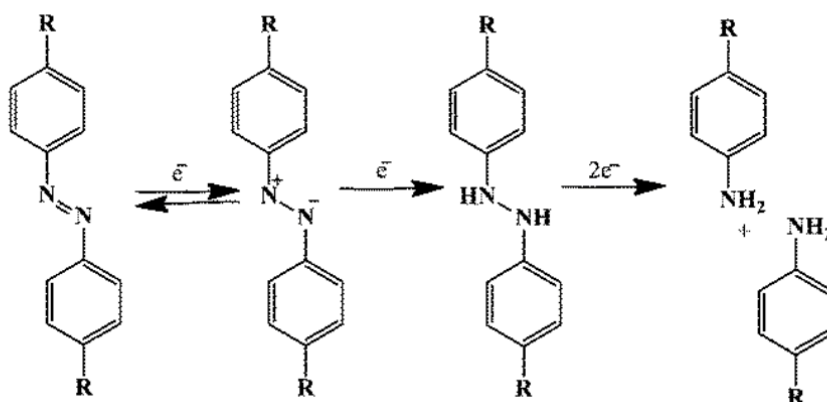

Figure 1.2: Reduction of Azobenzene Derivative's Nitrogen Double Bond into Two Amino Groups in a Reducing

Environment[9]

Azobenzene derivatives have seen extensive applications in the field of tumor targeting, particularly with respect to hypoxia-responsiveness. Kulkarni et al. developed an azo derivative diblock copolymer that self-assembles in aqueous solutions and specifically targets pancreatic cancer cells. To simulate a reducing environment, the authors conducted *in vitro* studies using nitrogen gas. The nanocapsules effectively released anticancer drugs at hypoxic tumor sites without any significant release in non-tumorous cell regions.[10] Sun et al. created a covalently self-

---

[9] Thambi, T., Park, J. H., & Lee, D. S. (2016). Hypoxia-responsive nanocarriers for cancer imaging and therapy: recent approaches and future perspectives. Chemical Communications, 52(55), 8492–8500.
[10] Kulkarni, P., Haldar, M. K., You, S., Choi, Y., & Mallik, S. (2016, July 1). Hypoxia-Responsive Polymersomes for Drug Delivery to Hypoxic Pancreatic Cancer Cells. Biomacromolecules, 17(8), 2507–2513.

assembled nanocapsule structure through direct crosslinking and showcased its efficacy in drug delivery to cancer cells. The researchers simulated a hypoxic environment by placing a glass barrier over the cancer cells, which obstructed oxygen diffusion and created an oxygen gradient. Their *in vivo* experiments using zebrafish embryos further validated the hypoxia-responsive drug release.[11] Shen et al. prepared noncovalently bonded fluorescent probes that could target tumor cells and undergo controlled activation of fluorescence when fluorescent probes were reduced by reductive enzymes, highlighting its potential applications in advanced bioimaging.[12]

Current methods for grafting azobenzene onto hyaluronic acid typically result at a low grafting ratio due to the significant steric hindrance presented by the azobenzene group. For example, Rosales et al. prepared hydrogels by grafting azobenzene and cyclodextrin onto hyaluronic acid using a direct esterification reaction, which achieved a grafting ratio of only approximately 30%[13]. A suboptimal grafting ratio can adversely affect the material's self-assembly and hypoxia-responsive efficiencies. Therefore, devising an efficient method with a higher grafting rate is crucial for advancing this field of study.

[11] Sun, C., Yue, L., Cheng, Q., Wang, Z., & Wang, R. (2020, February 12). Macrocycle-Based Polymer Nanocapsules for Hypoxia-Responsive Payload Delivery. ACS Materials Letters, 2(3), 266–271.

[12] Shen, J., Xue, T., & He, Y. (2020, June 9). An Enzyme-Activable Noncovalent Fluorescent Probe Based on Water Soluble Azobenzene Containing Polymer and AIEgen. Macromolecular Chemistry and Physics, 221(13).

[13] Rosales, A. M., Rodell, C. B., Chen, M. H., Morrow, M. G., Anseth, K. S., & Burdick, J. A. (2018, February 6). Reversible Control of Network Properties in Azobenzene-Containing Hyaluronic Acid-Based Hydrogels. Bioconjugate Chemistry, 29(4), 905–913.
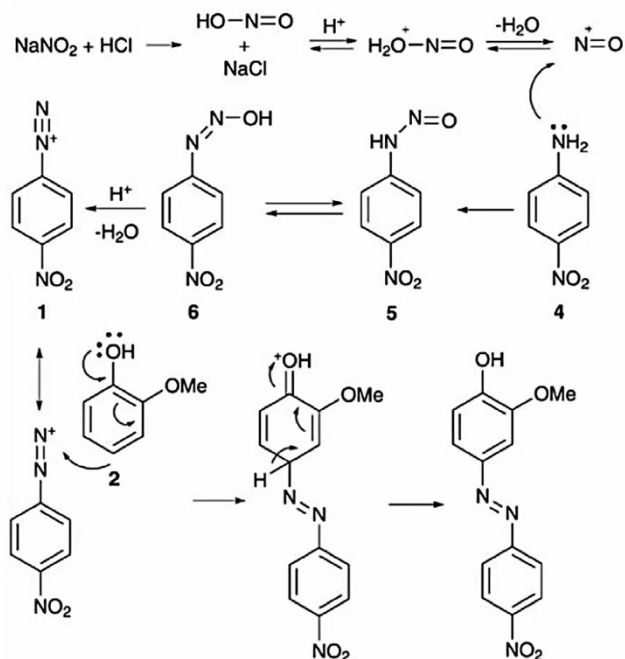
Figure 1.3: Azo-coupling Reaction Scheme[14]

Rather than directly linking the azobenzene group to hyaluronic acid, the synthesis of azobenzene onto hyaluronic acid can largely circumvent the issue of significant steric hindrance. Azo-coupling is a primary method for azobenzene synthesis, notable for its short reaction time, high yield, and high grafting ratio. As such, it stands out as a promising approach for creating hyaluronic acid based azo polymers.

In azo-coupling, a primary aromatic amine undergoes diazotization to form an aryl diazonium salt. This salt, acting as an electrophile, reacts with an electron-rich aromatic hydrocarbon, typically possessing an electron-donating group such as an amine or hydroxyl group, resulting in azobenzene. The main site for substitution reaction in azo-coupling is usually the para-position of

[14] Cheng, H., Zhang, S., Qi, J., Liang, X., & Yoon, J. (2021, May 24). Advances in Application of Azobenzene as a Trigger in Biomedicine: Molecular Design and Spontaneous Assembly. Advanced Materials, 33(26).

the electron-rich aromatic ring, but if the para-position is already occupied, the ortho-position can be an alternative reaction site.

The choice of reactant in azo-coupling influences the solution's acidity. When a phenolic compound is the reactant, the reaction usually needs to be carried out in a weakly basic environment. In contrast, when an aromatic amine compound is used, a weakly acidic condition is preferable. Therefore, controlling the acidity of the reaction environment is essential during the azo-coupling reaction.[15,16]

This research employed azo-coupling to graft azobenzene onto hyaluronic acid, aiming for a higher grafting ratio and faster reaction rate. This study utilized the following methodology. First, hyaluronic acid was reacted with tetrabutylammonium hydroxide to make hyaluronic acid (HA) soluble in organic solvents. Then, functional groups conducive to azo-coupling were grafted onto hyaluronic acid via a transesterification reaction. Lastly, Hyaluronic based azo polymer (HA-Azo-COOH) was synthesized through azo-coupling reaction in order to obtain a polymer with a high grafting ratio. ^{1}H NMR was used to characterize the products from each synthesis step. Subsequently, the polymer underwent self-assembly in selected solvents (DMSO/H_2O) to form colloidal spheres that were then characterized using dynamic light scattering instrument(DLS) and transmission electron microscopy(TEM). Finally, the redox-responsiveness and payload release capabilities of the polymer were validated introducing sodium dithionite to the product solution to

[15] Merino, E. (2011). Synthesis of azobenzenes: the coloured pieces of molecular materials. Chemical Society Reviews, 40(7), 3835.
[16] Cheng, H., Zhang, S., Qi, J., Liang, X., & Yoon, J. (2021, May 24). Advances in Application of Azobenzene as a Trigger in Biomedicine: Molecular Design and Spontaneous Assembly. Advanced Materials, 33(26).

simulate the reducing environment and using UV-Vis spectroscopy and fluorescence spectroscopy to characterize the results.

2. Experimental Section

2.1 Materials

Reagent	Molecular Formula	Purity	Brand
Hyaluronic Acid	$(C_{14}H_{21}NO_{11})_n$	(MW 9000)	HenghuiBio
Tetrabutylammonium Hydroxide	$C_{16}H_{37}NO$	40%W/W aqueous solution	Meryer
N-Ethyl-N-Hydroxyethylbenzene	$C_{10}H_{15}NO$	99%	Meryer
p-Toluenesulfonyl chloride	$C_7H_7ClO_2S$	99%	J&K Scientific
Tetrahydrofuran	C_4H_8O	AR	Greagent
Potassium Hydroxide	KOH	85%	J&K Scientific
Potassium Carbonate	K_2CO_3	AR	Greagent
Dimethyl Sulfoxide	C_2H_6OS	99%	Meryer
Aminobenzoic acid	$C_7H_7NO_2$	99%	J&K Scientific
Sodium Hydroxide	NaOH	AR	Greagent
Conc. Hydrochloric Acid	HCl	GR	Tong Guang
Sodium Nitrite	$NaNO_2$	99%	Meryer
Petroleum Ether	/	AR	Greagent

Ethyl Acetate	$C_4H_8O_2$	AR	Tong Guang
Sodium Chloride	NaCl	99%	Adamas
Sodium Dithionite	$Na_2S_2O_4$	88%	Meryer
1-(4-Aminophenyl)-1,2,2-triphenylethene	$C_{26}H_{21}N$	98%	Cercis Chemical
Deionized Water	H_2O	/	/

Table 1: Major Materials

2.2 Instruments

Instrument	Type	Manufacturer
^{1}H NMR Spectrometer	JOEL spectrometer (JNM-ECZ400S)	JOEL
Transmission Election Microscope	TEM H7650-B	HITACHI
Dynamic Light Scattering Instrument	ZSU3200	MALVERN Zetasizer
UV-Vis Spectrometer	Agilent Cary 300	Agilent Technologies
Fluorescence Spectrometer	F-7000	HITACHI

Table 2: Major Instruments

2.3 Methodology

2.3.1 Synthesis of HA-Azo-COOH

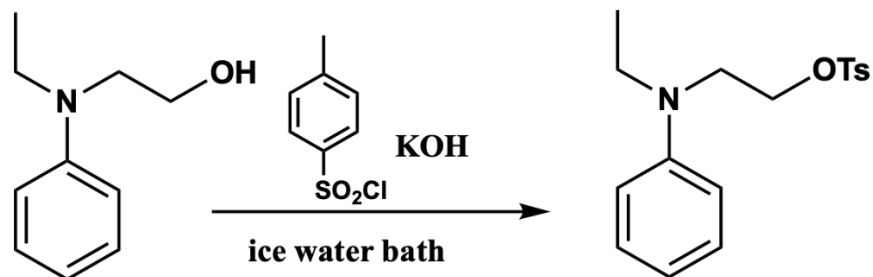**Preparation of *N*-Ethyl-*N*-(ethyl 4-methylbenzenesulfonate) aniline (NBNE)**

Figure 2.1: Preparation of NBNE

3.321 g of *N*-ethyl-*N*-hydroxyethylbenzene and 4.223 g of *p*-toluenesulfonyl chloride were dissolved in 70 mL tetrahydrofuran (THF) and the mixture was stirred at 0°C in an ice-water bath. Separately, 1.273 g of potassium hydroxide was dissolved in water within an ice-water bath, which was subsequently added to the THF mixture and stirred continuously for 24 hours. During this period, a noticeable color change from clear to light green was observed. Next, 700 mL of petroleum ether was introduced to the stirred mixture, and the solution turned cloudy. The solution was then subjected to extraction and separation using saturated sodium chloride, and magnesium sulfate was used to further eliminate water molecules. After crystallizing the solution at -18°C for 24 hours, petroleum ether was decanted. The remaining solution underwent lyophilization in a vacuum oven for 12 hours. This process yielded 3.200 g of a white solid, representing a 48% yield.

Preparation of Hyaluronic Acid Tetrabutylammonium Hydroxide Salt (HA-TBA)
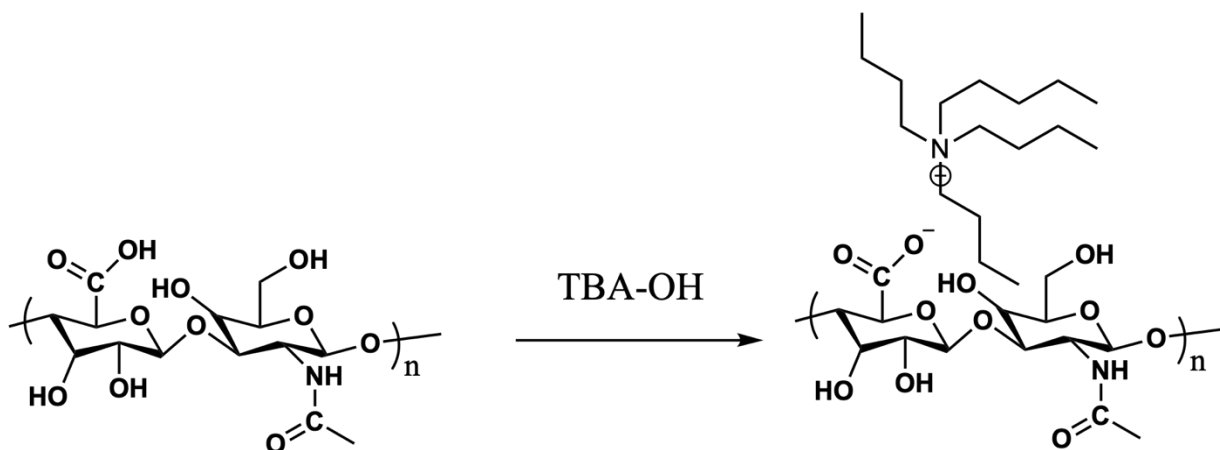
Figure 2.2: Preparation of HA-TBA

2.300 g of hyaluronic acid was dissolved in 100 mL of deionized water, and 12.484 g of tetrabutylammonium hydroxide (40% w/w aqueous solution) was added to this solution. The mixture was allowed to react for 12 hours, and dialysis of the solution was then performed in water for 24 hours to treat the product. Subsequently, the solution was crystallized using liquid nitrogen and then held in a freeze dryer for 70 hours. This process yielded 2.343 g of white, cotton-like HA-TBA, representing a 60% yield.

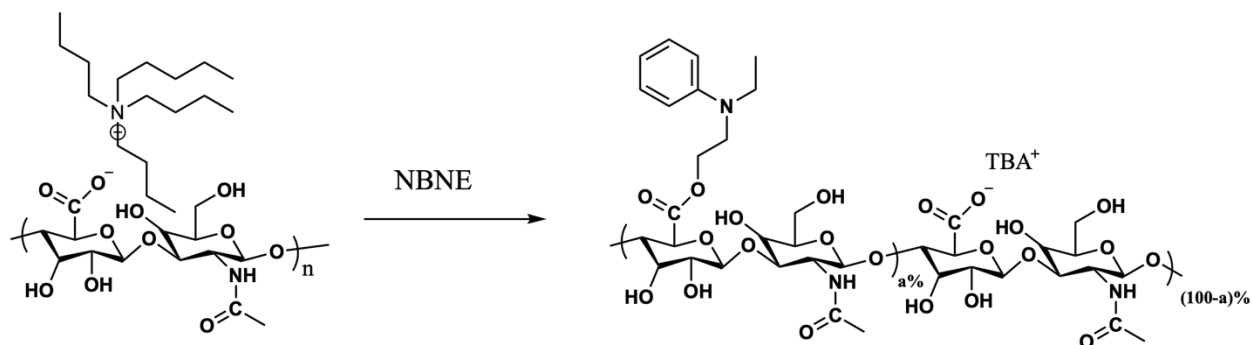**Preparation of Benzene Modified Hyaluronic Acid (HA-NE)**

Figure 2.3: Preparation of HA-NE

1.232 g HA-TBA was first dissolved in 80 mL of DMSO. Subsequently, 2.500 g of NBNE and 0.570 g of potassium carbonate was added into the solution. After being reacted for 24 hours, a visible color change was gradually being observed from clear to red. After reacting for 3 days, petroleum ether and ethyl acetate (in 1:1 ratio) were added to extract HA-NE, and dialysis of the solution was performed in water for 24 hours to treat the product. Subsequently, the solution was crystallized using liquid nitrogen and then held in a freeze dryer for 70 hours. The process yielded 0.405 g of a light-yellow, cotton-like substance, representing a 39% yield.

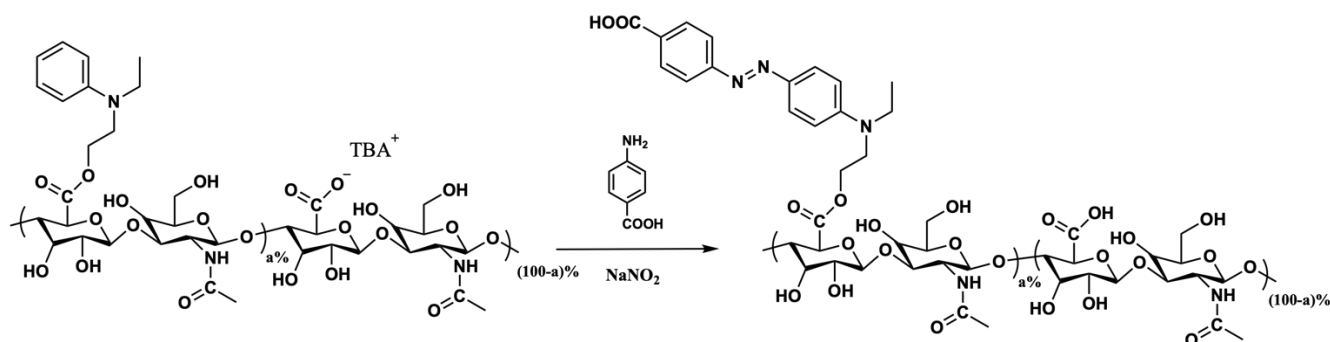**Preparation of Hyaluronic Acid Based Azo Polymer (HA-Azo-COOH)**

Figure 2.4: Preparation of Ha-Azo-COOH

The synthesis involved two primary steps. First, the diazonium salt was prepared. A solution was prepared by dissolving 0.55 g of aminobenzoic acid and 0.16 g of NaOH in 5 mL of water, maintained in an ice water bath. While stirring, 1.12 mL of concentrated hydrochloric acid was first added into the solution, followed by excess sodium nitrite (0.336 g). The solution quickly turned from clear to light yellow. For the second step, 0.41 g HA-NE was dissolved in 80 mL DMSO. While stirring, the diazonium salt prepared from the previous step was added dropwise into the HA-NE solution. After reacting at room temperature for 12 hours, a noticeable color

15

change was observed from clear to red. Petroleum ether and ethyl acetate (in a 1:1 ratio) were added to extract HA-Azo-COOH and dialysis of the solution was performed in water for 72 hours to treat the product. Subsequently, the solution was crystallized using liquid nitrogen and then held in a freeze dryer for 70 hours. The process resulted in a 56% yield.

2.3.2 Preparation of Self-Assembled Colloidal Spheres

The self-assembly of HA-Azo-COOH into colloidal spheres is primarily influenced by its amphiphilic nature. The hydrophobic parts of the polymer tend to be encapsulated in the center, while the hydrophilic parts tend to orient themselves on the external surface. As a result, this organization prompts the polymer to self-assemble into spherical structures in selected solvent.

To initiate the process, 1.2 mL of 3.5 mg/mL HA-Azo-COOH was transferred to a 10 mL round-bottom flask. Subsequently, deionized water (5 mL) was gradually dropped into the HA-Azo-COOH solution using a syringe at a constant rate of 7.2 mL/h, all while maintaining continuous stirring.

2.3.3 Characterization of HA-Azo-COOH

The synthesis of HA-Azo-COOH was monitored at each step using ^{1}H NMR spectroscopy. This allowed for both structural observation of the product and calculation of the grafting ratios. After undergoing self-assembly, the average particle size and distribution of colloidal spheres were assessed using a DLS instrument, while TEM was used to captured images of the spheres from the same batch.

2.3.4 Characterization of Redox-Responsiveness and Simulation of Payload Release

To characterize the redox-responsiveness and the payload release capability of the colloidal spheres, HA-Azo-COOH was initially co-assembled with amine-functionalized tetraphenylethene (TPE-NH$_2$). A 1.5 mL solution of 3 mg/mL HA-Azo-COOH was mixed with 200 μL of 10 mg/mL TPE-NH$_2$. Subsequently, 5 mL of deionized water was dropped into the mixed solution using a syringe at a rate of 7.2 mL/h while stirring at 800 rpm. TPE-NH$_2$ is an aggregation-induced emission probe that is highly hydrophobic.[17] Due to its hydrophobic nature, TPE-NH$_2$ will be sequestered within the interior of HA-Azo-COOH during the self-assembly process. The resulting spheres were characterized with TEM. The absorption and fluorescence peaks of the combined HA-Azo-COOH and TPE-NH$_2$ solution were determined using UV-Vis and fluorescence spectroscopy, respectively. Then, 4 mg of sodium dithionite was added to the HA-Azo-COOH and TPE-NH$_2$ solution and absorption and fluorescence peaks were subsequently measured again with UV-Vis spectroscopy and fluorescence spectroscopy.

3. Results and Discussion

3.1 Preparation and Characterization of HA-Azo-COOH

Hyaluronic acid has numerous carboxyl groups that facilitate its modification via azo-coupling reactions. A modified polymer was synthesized in three main parts, each characterized by ^{1}H NMR spectroscopy for both structure and grafting ratio. First, since hyaluronic acid is highly hydrophilic

---

[17] Chatterjee, A., Khandare, D. G., Saini, P., Chattopadhyay, A., Majik, M. S., & Banerjee, M. (2015). Amine functionalized tetraphenylethylene: a novel aggregation-induced emission based fluorescent chemodosimeter for nitrite and nitrate ions. RSC Advances, 5(40), 31479–31484.

and insoluble in most organic reagents, it was treated with tetrabutylammonium hydroxide through an acid-base neutralization reaction, ensuring its solubility in DMSO. The ^{1}H NMR spectrum of HA-TBA were taken (Figure 3.1), and the areas of peak a and peak b were calculated as S_a and S_b. The grafting ratio for this step was calculated as $\frac{S_b/4}{S_a}$, giving approximately 100%.

For the second step of synthesis, HA-NE was obtained by grafting NBNE on HA-TBA through a transesterification reaction in order to provide a functional group that is capable of azo-coupling reactions. The ^{1}H NMR spectrum of HA-NE were taken (Figure 3.2), and the integrations of peaks a-d were calculated. The grafting ratio for this step was calculated as $\frac{(S_b+S_c+S_d)/5}{S_a/3}$, giving approximately 80%.

The final product was prepared by azo-coupling from diazonium salt and HA-NE. The ^{1}H NMR spectrum for HA-Azo-COOH was taken (Figure 3.3), and the integrations for peaks a-e were calculated. The grafting ratio for this step was then calculated as $\frac{(S_c+S_d+S_e+S_f)/8}{S_b/3}$, giving approximately 75%.

Using azo-coupling, the grafting ratio increased by 45%, an improvement from the previous 30% achieved through the esterification reaction. A higher grafting ratio potentially enhances the material's self-assembly efficiency and redox-responsive efficiency. However, the yields at each synthesis stage remained relatively low, at 48%, 60%, 39%, and 56% respectively. A significant contributing factor to these low yields is the extended dialysis time required for product treatment. Shortening the dialysis duration could increase yield, but this might also lead to a rise in impurities. Therefore, striking an optimal balance between yield and purity is essential when synthesizing the

polymer. Future experiments could explore modifications in reaction conditions in order to further optimize the preparation yield.
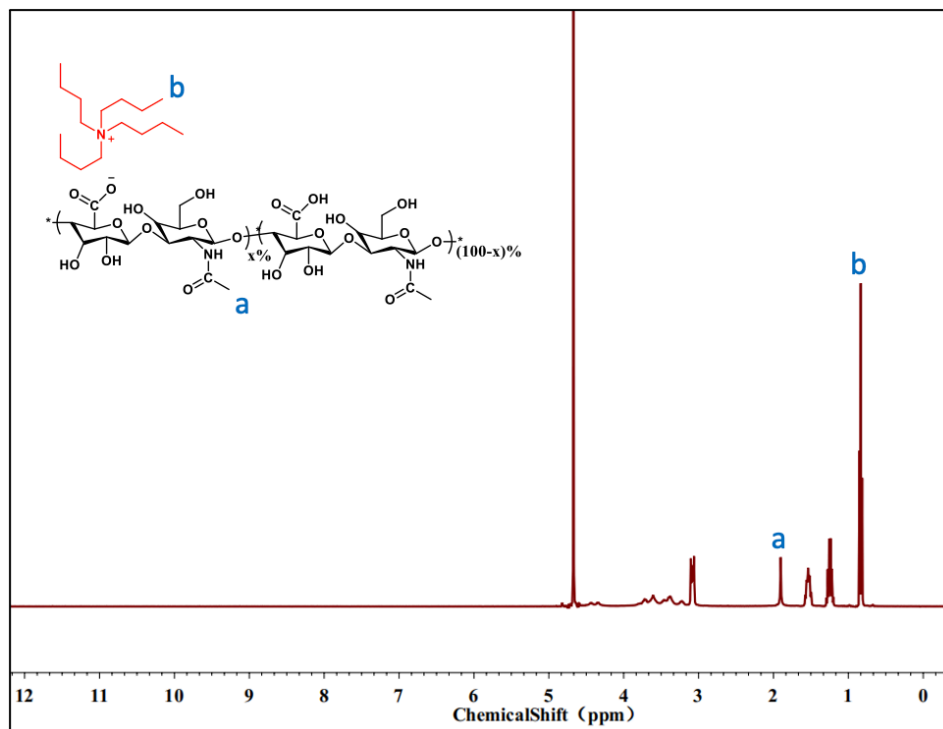

Figure 3.1: ^{1}H NMR Spectrum of HA-TBA[18]

---

[18] D_2O is the solvent, a represents the chemical shift of the methyl group in hyaluronic acid, and b represents the chemical shift of the methyl group in tetrabutylammonium hydroxide.
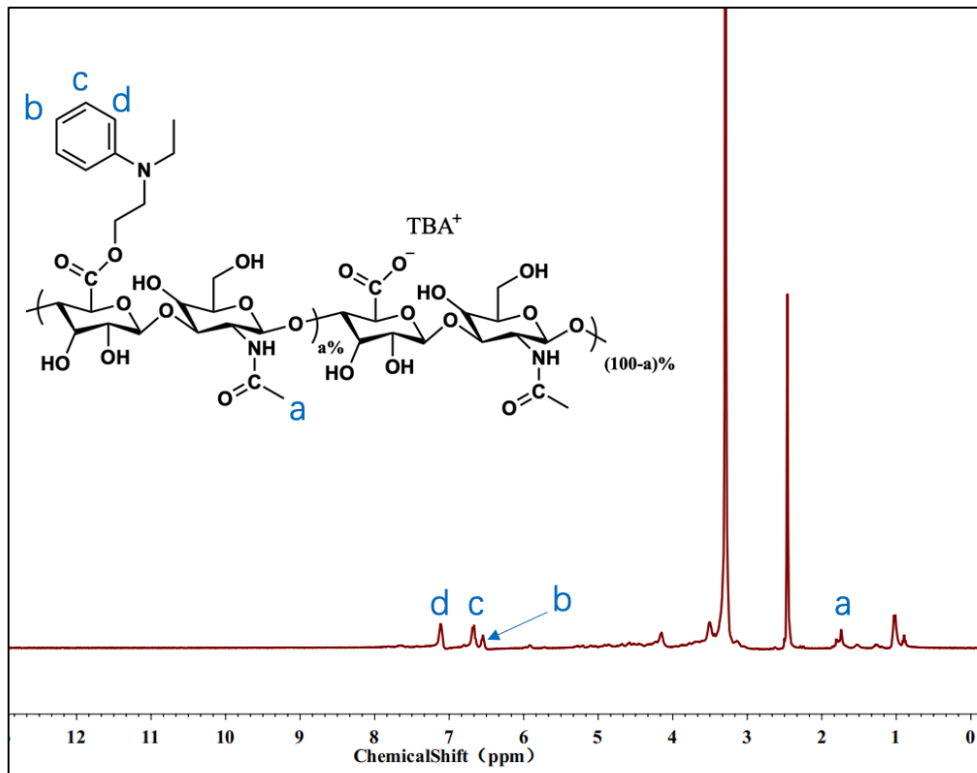
Figure 3.2: ^{1}H NMR Spectrum of HA-NE[19]

---

[19] Deuterated DMSO is the solvent, a represents the chemical shift of the methyl group in hyaluronic acid, and b, c, d each represent chemical shifts of hydrogen atoms on the benzene ring, respectively.
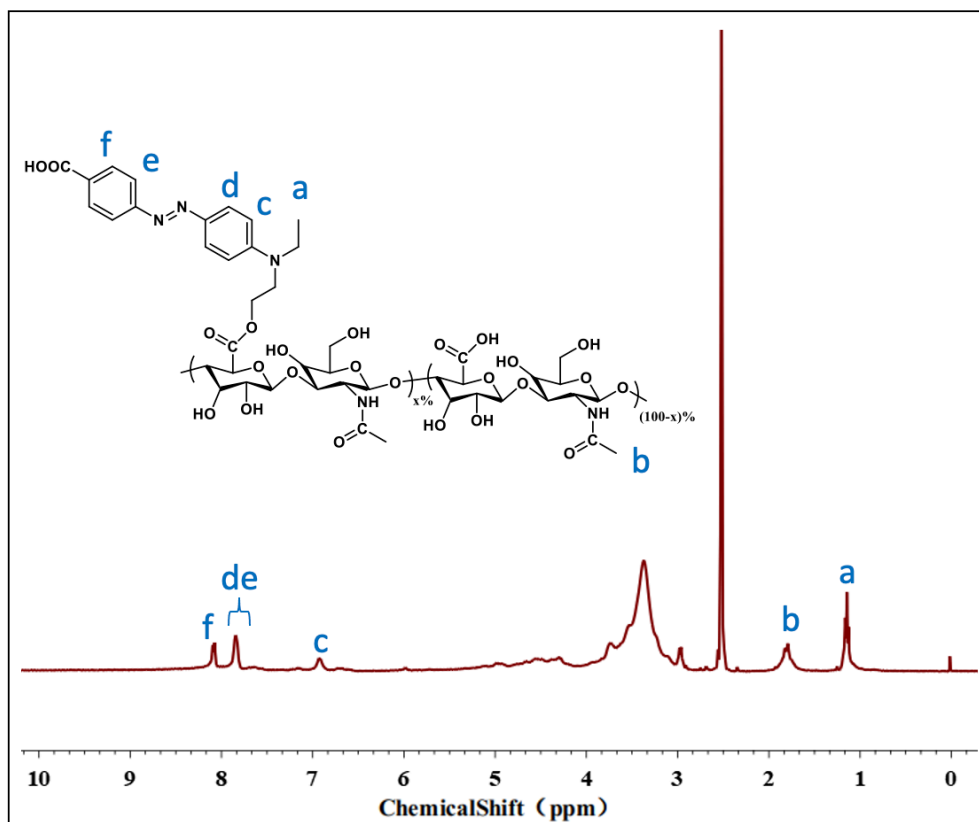
Figure 3.3: ^{1}H NMR Spectrum of HA-Azo-COOH[20]

3.2 Characterization of Self-Assembled Colloidal Sphere

Nano colloidal spheres offer a wide range of promising applications, especially as targeted drug carriers.[21,22] A common method of preparing nano colloidal spheres involves allowing amphiphilic polymers to self-assemble in a designated solvent. The HA-Azo-COOH synthesized in this study possessed both hydrophilic and hydrophobic functional groups. Thus, when deionized

[20] Deuterated DMSO is the solvent, a represents the chemical shift of the methyl group in azobenzene, b represents the chemical shift of the methyl group in hyaluronic acid, and c-f each represent chemical shifts of hydrogen atoms on azobenzene, respectively.

[21] Fan, Y., Liu, Y., Wu, Y., Dai, F., Yuan, M., Wang, F., Bai, Y., & Deng, H. (2021, December). Natural polysaccharides based self-assembled nanoparticles for biomedical applications – A review. International Journal of Biological Macromolecules, 192, 1240–1255.

[22] Singamaneni, S., Bliznyuk, V. N., Binek, C., & Tsymbal, E. Y. (2011). Magnetic nanoparticles: recent advances in synthesis, self-assembly and applications. Journal of Materials Chemistry, 21(42), 16819.

water was added to the HA-Azo-COOH solution at an appropriate rate, the linear polymer chains began to coalesce into spherical structures due to amphiphilic interactions.

Using DLS instrument, as shown in Figure 3.4 (a), the average diameter of the self-assembled HA-Azo-COOH spheres was determined to be approximately 258 nm with a polydispersity index (PDI) of approximately 0.06. The TEM image of the same sample batch is presented in Figure 3.4 (b), which reveals well-defined boundaries and intact spherical structures, underscoring the successful self-assembly of the spheres.
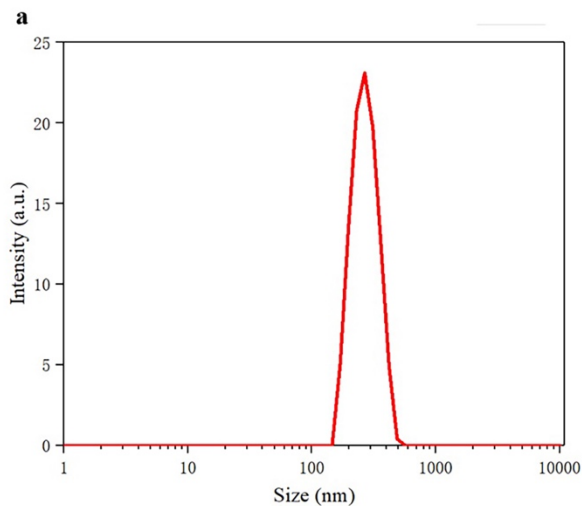

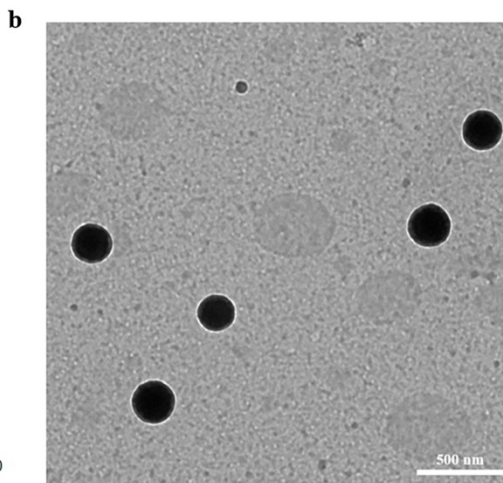Figure 3.4 (a): DLS of HA-Azo-COOH[23]   Figure 3.4 (b): TEM of HA-Azo-COOH[24,25]

3.3 Characterization of Redox-Responsiveness and Simulation of Payload Release

---

[23] After data processing, the PDI is approximately 0.06, and the diameter is approximately 258 nm.
[24] TEM image of nanospheres with a particle size of approximately 250 nm.
[25] During the preparation of TEM samples, the self-assembled HA-Azo-COOH solution was dropped onto a copper grid coated with carbon film and then dried at 25°C for 24 hours.
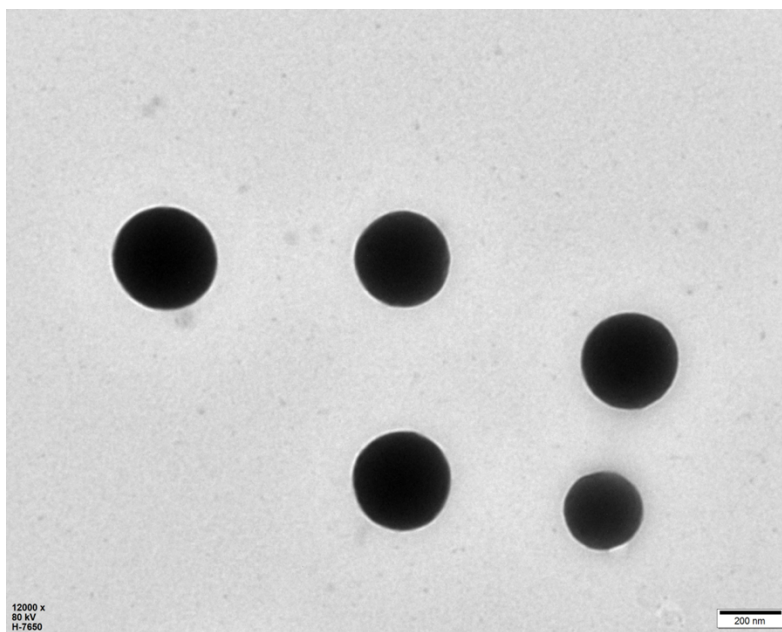
Figure 3.5: TEM Image of Self Assembled HA-Azo-COOH Colloidal Spheres With TPE-NH$_2$

Following the preparation of the HA-Azo-COOH and TPE-NH$_2$ colloidal spheres, TEM imaging confirmed their successful self-assembly with uniform colloidal spheres shown in Figure 3.5. In Figure 3.6, as demarcated by the red line and arrow, an absorption peak is evident at approximately 450 nm. This peak corresponds to the absorption of the nitrogen-nitrogen double bond present in HA-Azo-COOH. The blue line depicts the absorption characteristics of the colloidal spheres after reduction by sodium dithionite. Notably, the azo absorption peak at 450 nm is no longer present, suggesting that the nitrogen-nitrogen double bond in azobenzene has been reduced, resulting in its cleavage into two amino groups. Such a change in the structure of azobenzene can destabilize the overall structure of the self-assembled spheres, underscoring the redox-responsive nature of the material.
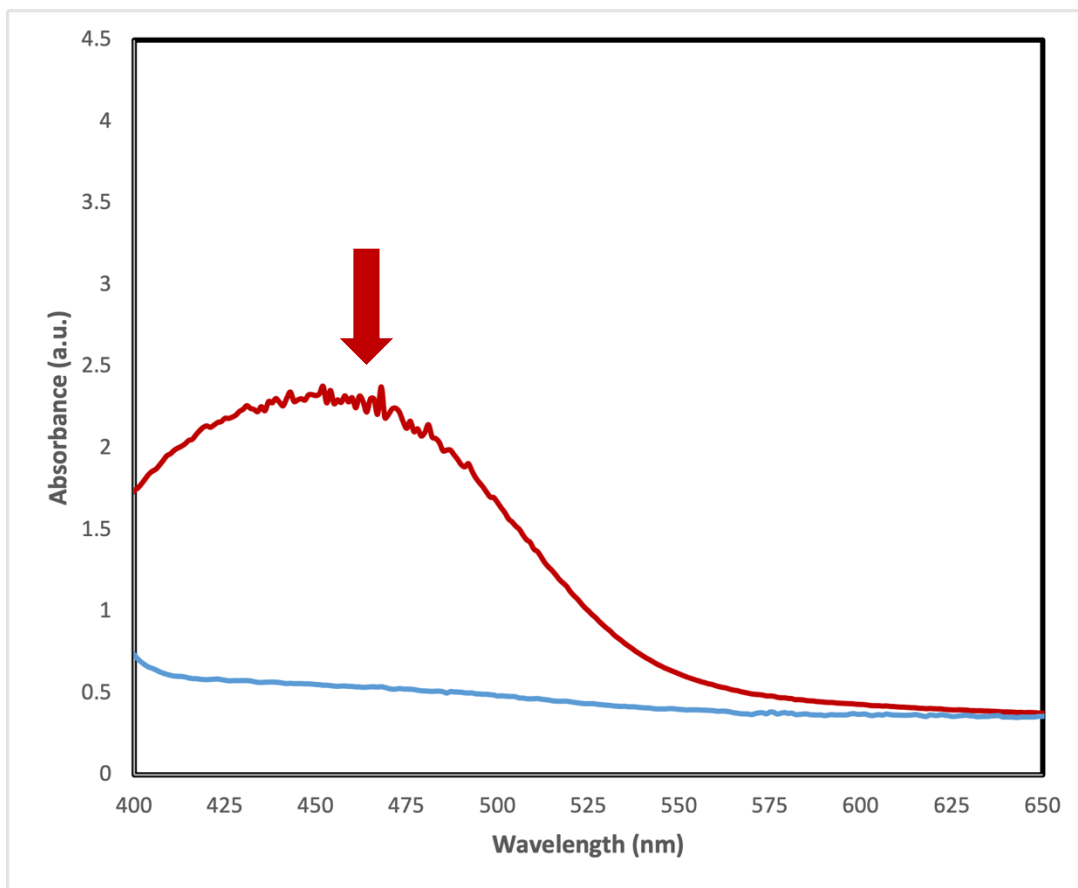
Figure 3.6: UV-Vis Absorption Spectrum of HA-Azo-COOH Before (Red Line) and After (Blue Line) Sodium Dithionite

Addition

TPE-NH$_2$ was used to simulate payload drugs. When it was encapsulated by HA-Azo-COOH, the absorption peak of azobenzene quenched the fluorescence of TPE-NH$_2$. As shown with the blue line in Figure 3.7, there is no apparent fluorescence peak. However, upon the reduction of azobenzene by sodium dithionite, leading to the disruption of the HA-Azo-COOH structure, TPE-NH$_2$ was released into deionized water. Given the nature of TPE-NH$_2$ as an aggregation-induced emission fluorescent probe, it aggregates in water and emits intense fluorescence, as manifested by a prominent fluorescence peak at 480 nm indicated by the red line in Figure 3.7. These findings

demonstrate that the material possesses redox-responsive properties, enabling it to encapsulate hydrophobic payloads and release them in a reducing environment.
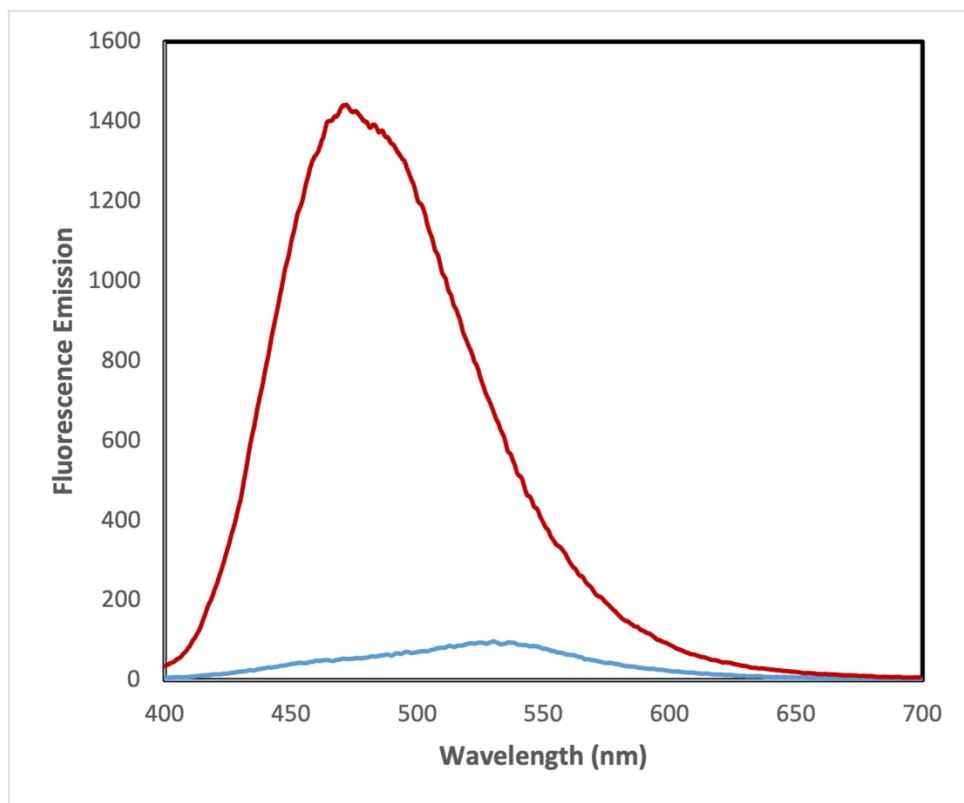

Figure 3.7: Fluorescence Spectrum of HA-Azo-COOH and TPE-NH$_2$ solution (Blue line: before; Red line: sodium dithionite is

added; Excitation Wavelength: 365 nm)

4. Conclusion

In this study, carboxyl-azobenzene was grafted onto hyaluronic acid via an azo-coupling reaction. First, the carboxyl group in hyaluronic acid was modified using tetrabutylammonium hydroxide, enhancing its solubility in organic solvents. This modified hyaluronic acid was then reacted with NBNE to introduce a functional group that is capable of azo-coupling. In the final

step, the diazonium salt derived from aminobenzoic acid was employed to successfully graft carboxyl-azobenzene onto hyaluronic acid. This methodology resulted in a high degree of functionalization for hyaluronic acid, achieving an azobenzene grafting ratio of 75%. This represents a significant enhancement compared to the previous grafting ratio of approximately 30% obtained from esterification reactions[26].

Uniform and stable colloidal spheres were prepared by optimizing the conditions for HA-Azo-COOH self-assembly in the chosen solvent. The introduction of a reducing agent led to the notable disappearance of the azobenzene absorption peak in the UV-Vis spectrum. This observation confirms that the nitrogen-nitrogen double bond in azobenzene can be efficiently reduced to yield two distinct amino groups, thereby highlighting the redox-responsiveness of HA-Azo-COOH.

Using fluorescence spectroscopy and TPE-NH$_2$ as a model, the payload process was successfully simulated. This demonstration underlines the potential of HA-Azo-COOH as a carrier for tumor cell-targeting drugs. For future study, refinements for reaction conditions to further enhance yield should be done. *In vitro* testing with cells and anticancer drugs will be crucial to ascertain the material's toxicity and efficacy in precisely targeting and killing the tumor cells while sparing healthy ones. *In vivo* studies using laboratory mice should also be performed to further investigate the material's potential as a targeted cancer drug delivery system.

---

[26] Rosales, A. M., Rodell, C. B., Chen, M. H., Morrow, M. G., Anseth, K. S., & Burdick, J. A. (2018, February 6). Reversible Control of Network Properties in Azobenzene-Containing Hyaluronic Acid-Based Hydrogels. Bioconjugate Chemistry, 29(4), 905–913.

5. References

1. Bawa, P., Pillay, V., Choonara, Y. E., & du Toit, L. C. (2009, March 5). Stimuli-responsive polymers and their applications in drug delivery. Biomedical Materials, 4(2), 022001. https://doi.org/10.1088/1748-6041/4/2/022001

2. Bicudo, R. C. S., & Santana, M. H. A. (2012, March 1). Effects of Organic Solvents on Hyaluronic Acid Nanoparticles Obtained by Precipitation and Chemical Crosslinking. Journal of Nanoscience and Nanotechnology, 12(3), 2849–2857. https://doi.org/10.1166/jnn.2012.5814

3. Chatterjee, A., Khandare, D. G., Saini, P., Chattopadhyay, A., Majik, M. S., & Banerjee, M. (2015). Amine functionalized tetraphenylethylene: a novel aggregation-induced emission based fluorescent chemodosimeter for nitrite and nitrate ions. RSC Advances, 5(40), 31479–31484. https://doi.org/10.1039/c4ra14765k

4. Cheng, H., Zhang, S., Qi, J., Liang, X., & Yoon, J. (2021, May 24). Advances in Application of Azobenzene as a Trigger in Biomedicine: Molecular Design and Spontaneous Assembly. Advanced Materials, 33(26). https://doi.org/10.1002/adma.202007290

5. Fan, Y., Liu, Y., Wu, Y., Dai, F., Yuan, M., Wang, F., Bai, Y., & Deng, H. (2021, December). Natural polysaccharides based self-assembled nanoparticles for biomedical applications – A review. International Journal of Biological Macromolecules, 192, 1240–1255. https://doi.org/10.1016/j.ijbiomac.2021.10.074

6. Klemm, D., Heublein, B., Fink, H. P., & Bohn, A. (2005, May 30). Cellulose: Fascinating Biopolymer and Sustainable Raw Material. Angewandte Chemie International Edition, 44(22), 3358–3393. https://doi.org/10.1002/anie.200460587

7. Kulkarni, P., Haldar, M. K., You, S., Choi, Y., & Mallik, S. (2016, July 1). Hypoxia-Responsive Polymersomes for Drug Delivery to Hypoxic Pancreatic Cancer Cells. Biomacromolecules, 17(8), 2507–2513. https://doi.org/10.1021/acs.biomac.6b00350

8. Luo, Z., Dai, Y., & Gao, H. (2019, November). Development and application of hyaluronic acid in tumor targeting drug delivery. Acta Pharmaceutica Sinica B, 9(6), 1099–1112. https://doi.org/10.1016/j.apsb.2019.06.004

9. Merino, E. (2011). Synthesis of azobenzenes: the coloured pieces of molecular materials. Chemical Society Reviews, 40(7), 3835. https://doi.org/10.1039/c0cs00183j

10. Rosales, A. M., Rodell, C. B., Chen, M. H., Morrow, M. G., Anseth, K. S., & Burdick, J. A. (2018, February 6). Reversible Control of Network Properties in Azobenzene-Containing Hyaluronic Acid-Based Hydrogels. Bioconjugate Chemistry, 29(4), 905–913. https://doi.org/10.1021/acs.bioconjchem.7b00802

11. Roy, D., Cambre, J. N., & Sumerlin, B. S. (2010, January). Future perspectives and recent advances in stimuli-responsive materials. Progress in Polymer Science, 35(1–2), 278–301. https://doi.org/10.1016/j.progpolymsci.2009.10.008

12. Shen, J., Xue, T., & He, Y. (2020, June 9). An Enzyme-Activable Noncovalent Fluorescent Probe Based on Water Soluble Azobenzene Containing Polymer and AIEgen. Macromolecular Chemistry and Physics, 221(13). https://doi.org/10.1002/macp.202000126

13. Singamaneni, S., Bliznyuk, V. N., Binek, C., & Tsymbal, E. Y. (2011). Magnetic nanoparticles: recent advances in synthesis, self-assembly and applications. Journal of Materials Chemistry, 21(42), 16819. https://doi.org/10.1039/c1jm11845e

14. Stuart, M. A. C., Huck, W. T. S., Genzer, J., Müller, M., Ober, C., Stamm, M., Sukhorukov, G. B., Szleifer, I., Tsukruk, V. V., Urban, M., Winnik, F., Zauscher, S., Luzinov, I., & Minko, S. (2010, January 22). Emerging applications of stimuli-responsive polymer materials. Nature Materials, 9(2), 101–113. https://doi.org/10.1038/nmat2614

15. Sun, C., Yue, L., Cheng, Q., Wang, Z., & Wang, R. (2020, February 12). Macrocycle-Based Polymer Nanocapsules for Hypoxia-Responsive Payload Delivery. ACS Materials Letters, 2(3), 266–271. https://doi.org/10.1021/acsmaterialslett.0c00002

16. Thambi, T., Park, J. H., & Lee, D. S. (2016). Hypoxia-responsive nanocarriers for cancer imaging and therapy: recent approaches and future perspectives. Chemical Communications, 52(55), 8492–8500. https://doi.org/10.1039/c6cc02972h

17. Wei, M., Gao, Y., Li, X., & Serpe, M. J. (2017). Stimuli-responsive polymers and their applications. Polymer Chemistry, 8(1), 127–143. https://doi.org/10.1039/c6py01585a

18. Wilson, W. R., & Hay, M. P. (2011, May 24). Targeting hypoxia in cancer therapy. Nature Reviews Cancer, 11(6), 393–410. https://doi.org/10.1038/nrc3064

Acknowledgements

This research project began in the official Science Talent (Yingcai) Program, where I was supervised by Professor Yaning He at Tsinghua University. After I completed the Science Talent Program in November 2022, I continued with further research under Prof He's guidance. Throughout the process, Prof He has given my invaluable support, especially in finding my research direction and conducting the research at his lab. Moreover, Ms. Ejing Kong, my high school chemistry teacher, has encouraged me to investigate organic chemistry and given me insightful advice in manuscript preparation. I am immensely grateful for their help and support in every aspect during the past two years. This project would have been impossible without them.